11-30-2020

A Climatological Analysis of the Monsoon Break Following the Summer Monsoon Onset Over Luzon Island, Philippines

Lyndon Mark P. Olaguera

Jun Matsumoto

Hisayuki Kubota

Esperanza O. Cayanan

Flaviana D. Hilario

Received: 18 February 2019 | Revised: 21 November 2020 | Accepted: 25 November 2020

DOI: 10.1002/joc.6949

RESEARCH ARTICLE

International Journal of Climatology RMetS

A climatological analysis of the monsoon break following the summer monsoon onset over Luzon Island, Philippines

Lyndon Mark P. Olaguera[1,2,3] | **Jun Matsumoto**[1,4] | **Hisayuki Kubota**[4,5] | **Esperanza O. Cayanan**[6] | **Flaviana D. Hilario**[6]

[1]Department of Geography, Tokyo Metropolitan University, Tokyo, Japan

[2]Physics Department, Ateneo de Manila University, Quezon City, Philippines

[3]Regional Climate Systems Laboratory, Manila Observatory, Quezon City, Ateneo de Manila University Campus, Quezon City, Philippines

[4]Dynamic Coupling of Ocean-Atmosphere-Land Research Program, Japan Agency for Marine Earth Science and Technology, Yokosuka, Japan

[5]Faculty of Science, Department of Earth and Planetary Sciences, Hokkaido University, Sapporo, Japan

[6]Department of Science and Technology, Philippine Atmospheric, Geophysical and Astronomical Services Administration, Quezon City, Philippines

Correspondence
Lyndon Mark P. Olaguera, Physics Department, Ateneo de Manila University, Quezon City, Philippines
Email: lolaguera@ateneo.edu

Funding information
Japan International Cooperation Agency; Japan Science and Technology Agency; Japan Society for the Promotion of Science, Grant/Award Numbers: 21684028, 16H03116, 16H04053, 18058043, 19H00562, 26220202, 20K20328, 15KK0030, 25282085; Tokyo Metropolitan Government

Abstract

This study investigates the climatology of the monsoon break following the onset of the summer rainy season over Luzon Island (120–122.5°E, 13–22°N) in the Philippines from 1979–2017. The first post-onset monsoon break is remarkable in stations located over the north and central Luzon Island and occurs climatologically in early June. Composite analysis of the large-scale circulation features during the monsoon break period shows that this break is associated with the westward extension of the western North Pacific Subtropical High (WNPSH), which weakened the monsoon southwesterlies and induced enhanced low-level divergence over Luzon Island. The westward extension of the WNPSH may be facilitated by the phase change of the boreal summer intraseasonal oscillation (BSISO). About 59% (23/39) of the monsoon break cases occurred when suppressed convection, associated with the dry phases of the BSISO, is apparent over the western North Pacific. This suppressed convection favours the westward expansion of the WNPSH.

With the occurrence of the monsoon break in early summer, the seasonal march of the early summer monsoon over the Philippines can be divided into three phases: (1) the monsoon onset phase, which occurs between mid to late May under the influence of the westerly/southwesterly low-level winds, (2) the monsoon break phase, when rainfall decreases over Luzon Island in early June, and (3) the monsoon revival phase, when rainfall increases again due to the intrusion of monsoon southwesterlies over the Philippines. This study highlights the complex features of the summer monsoon onset and the impact of the WNPSH on the local climate of the Philippines in early summer.

KEYWORDS

Baiu/Mei-yu, monsoon break, monsoon onset, Philippines, summer monsoon, western North Pacific subtropical high

1 | INTRODUCTION

The Asian summer monsoon (ASM) is well known for its stepwise evolution, prominent subseasonal variabilities—active-break cycles in rainfall, and abrupt changes that has been documented in many studies (e.g., Matsumoto, 1992; Nakazawa, 1992; Yanai *et al.*, 1992; Murakami and Matsumoto, 1994; Matsumoto, 1995; Ueda *et al.*, 1995; Ueda and Yasunari, 1996; Lau and Yang, 1997; Wang and Xu, 1997; Wu and Wang, 2000, 2001; LinHo and Wang, 2002; Wu, 2002; Ueda, 2005; Hung and Hsu, 2008, among others). For instance, Nakazawa (1992) showed the phase-locking feature of the seasonal progression of the ASM in the annual cycle and identified two important stages of rainfall enhancement. According to his study, the first enhancement of rainfall appears over the Indian Ocean in late May to early June, while the second enhancement occurs rather abruptly in late July over the western North Pacific (WNP). Lau and Yang (1997) used the 6 mm·day^{-1} contour line of the pentad rainfall estimates from the global precipitation index data set to depict the northward and northeastward advance of the monsoon rain zones over Southeast Asia. They showed that the summer monsoon starts in the Philippine area from south to north in early to mid-May. Murakami and Matsumoto (1994), on the other hand, used the pentad mean outgoing longwave radiation (OLR) from 1975 to 1977 and 1979 to 1987 and defined the onset of the summer monsoon as the pentad when the 12-year mean OLR begins to lower the annual mean OLR. They showed that the onset of the summer monsoon season progresses from west to east in mid-May to mid-June over the Philippines before proceeding northeastward in mid to late July.

Wang and Xu (1997) documented the breaks in rainfall during the summer monsoon season over the WNP. They attributed these breaks to the arrival of the dry phase of the climatological intra-seasonal oscillation (CISO). Matsumoto (1997) also identified a break in the summer rainy season over the Indochina Peninsula using pentad mean rainfall over Thailand. Takahashi and Yasunari (2006) suggested that this break is associated with a quasi-stationary ridge that is induced by the interaction of the monsoon westerlies and the topography of the Indochina Peninsula. On the other hand, Chen *et al.* (2004) pointed out that the break in the East Asian Summer Monsoon (EASM) occurs during the transition from the Mei-yu to the tropical cyclone season. An earlier study by Lau *et al.* (1988) suggested that this break is due to the westward/northwestward shifting of the western North Pacific Subtropical High (WNPSH) over East Asia. So and Chan (1997) investigated the break in rainfall in South China from April to June using the rainfall data in Hong Kong. They found that the increase in convective clouds during the onset and active periods over the South China region leads to a reduction in solar radiation, decrease in temperature, and an increase in sea level pressure that are favourable for the westward intrusion of the WNPSH. Meanwhile, Ramage (1952) also documented a monsoon break over South China using the rainfall data from Hongkong, Lungchow, and Taiwan from late June to early July. He suggested that this is related with the northward migration of the WNPSH.

Located in the western rim of the Pacific Ocean, the Philippines is part of the ASM system and its agricultural sector relies heavily on monsoon activity. The start of the planting season, for example, over most parts of the country coincides with the onset of the summer monsoon. In general, the Philippines can be divided into three major island groups, Luzon (Northern Philippines), Visayas (Central Philippines), and Mindanao (Southern Philippines). Luzon Island is the largest island with many locations having heights well above 500 m, as shown in Figure 1. These mountain ranges along the eastern coast (Sierra Madre) and western coast (Cordillera and Zambales Mountain ranges) of Luzon Island induce monsoon blocking effects such that during the summer monsoon season, the areas along the eastern coast experience their dry season, whereas the areas along the western coast experience their wet season. The opposite occurs during the winter monsoon season. Because of this spatial contrast in rainfall, the stations located along the western (eastern) coast of the country are often used in

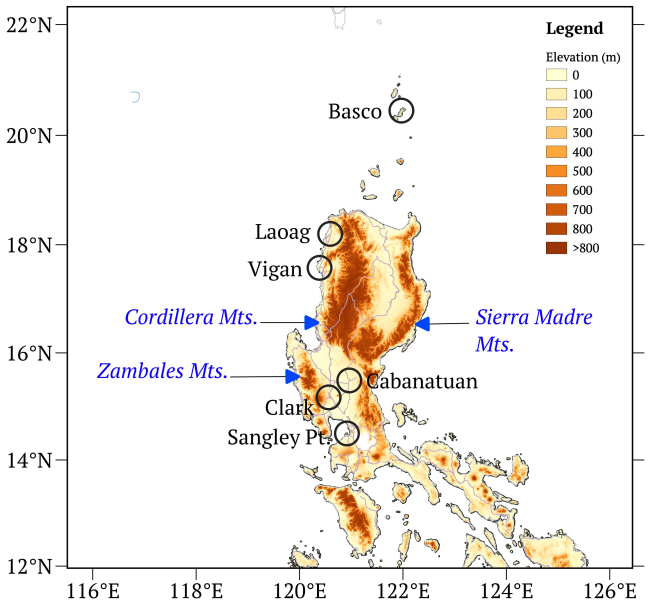

FIGURE 1 Location of the six meteorological stations from the Philippine atmospheric, geophysical and astronomical services administration (PAGASA) used in defining the monsoon break and the topography of the Philippines

defining the onset of the summer (winter) monsoon season (Kubota *et al*., 2017). Flores and Balagot (1969) noted that the summer monsoon over the Philippines originates as trades from the Indian Ocean Anticyclone during the Southern Hemisphere winter and reaches the country as southwesterlies. The summer monsoon onset over the country generally occurs between mid-May to late May and ends in October, although, sometimes, it may last until November or December (Flores and Balagot, 1969; Moron *et al*., 2009; Akasaka, 2010).

The rainfall of the Philippines is influenced by multi-scale systems such as the monsoons (Akasaka *et al*., 2007), the Inter-tropical Convergence Zone (ITCZ) (Yumul *et al*., 2011), the El Niño Southern Oscillation (ENSO) (Lyon and Camargo, 2009; Roberts *et al*., 2009), tropical cyclone activities (Cayanan *et al*., 2011; Kubota *et al*., 2017), the Intra-seasonal oscillations (ISO) (Pullen *et al*., 2015), the Pacific-Japan Pattern (Kubota *et al*., 2016), and the WNPSH (Flores and Balagot, 1969; LinHo and Wang, 2002). However, it is only recently that the impacts of these systems on the local climate of the Philippines have been elucidated compared to the adjacent regions (e.g., South China Sea [SCS], Indochina, and South Asia). For example, no onset date isolines are depicted in the classical textbooks such as Ramage (1971) or Tao and Chen (1987), although local onset maps are depicted by Asuncion and Jose (1980) using station-based rainfall.

While several studies such as Akasaka *et al*. (2007), Moron *et al*. (2009), Akasaka (2010), Cruz *et al*. (2013), and Matsumoto *et al*. (2020) have examined the onset, withdrawal, seasonal climatology, and regional differences of the summer monsoon over the Philippines, the important sub-seasonal variations (i.e., active-break cycle) during the life cycle of the summer monsoon season in the country are less emphasized in these studies. Therefore, the present study is our initial attempt to fill this research gap. In addition, an understanding of these sub-seasonal variations is important for a better understanding of the weather and climate variability of the Philippines.

This paper is organized as follows. The data and methodology used in this study are described in Section 2. We identify and characterize the monsoon break including its climatology through a composite analysis and the possible mechanism inducing it in Section 3. The discussions and summary are provided in Sections 4 and 5, respectively.

2 | DATA SOURCES AND METHODOLOGY

2.1 | Data

The primary datasets analysed in this study include:

1. Daily rainfall data at six meteorological stations (Basco, Laoag, Vigan, Clark, Cabanatuan, and Sangley Pt. stations) from the Philippine Atmospheric, Geophysical and Astronomical Services Administration (PAGASA), the country's official weather bureau from 1979 to 2017. These stations are shown in Figure 1 and their mean daily rainfall relative to the break of the rainy season provided by PAGASA is shown in Figure 2. All stations used in this study have less than 40% missing values from May to August season from 1979 to 2017, except for Clark Station, where the rainfall record started on July 1997.
2. Daily rainfall data from the Tropical Rainfall Measuring Mission Multi-Satellite Precipitation Analysis (TRMM-TMPA) 3B42 version 7 (Huffman and Bolvin, 2018), with 0.25° × 0.25° resolution from 1998 to 2015.
3. Daily reanalysis data, with 2.5° × 2.5° horizontal grid resolution, of zonal winds (*U*), meridional winds (*V*), geopotential height (*HGT*), temperature (*TEMP*), relative humidity (*RHUM*), vertical velocity (*OMEGA*), and specific humidity (*SHUM*) from the National Center for Environmental Prediction-Department of Energy (NCEP-DOE) Atmospheric Model Intercomparison Project (AMIP-II) Reanalysis (Kanamitsu *et al*., 2002) at multiple levels and from 1979 to 2017.

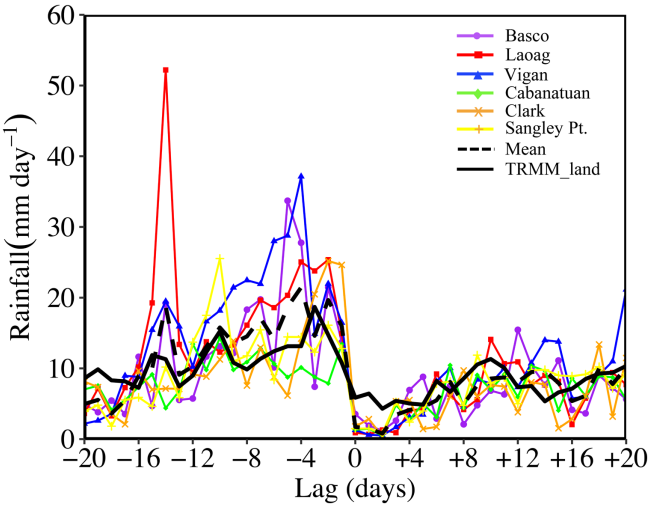

FIGURE 2 Lag composites of daily rainfall relative to the first day of the monsoon break period (Lag 0; 1979–2017; mm·day^{-1}) for the six stations used in defining the monsoon break period (Basco, Laoag, Vigan, Cabanatuan, Clark, Sangley Point), the average rainfall from these six stations (Mean; dashed line), and rainfall from TRMM (based on land points only; TRMM_land; black solid line; 1998–2015; mm·day^{-1}) averaged over Luzon Island (120–122.5°E, 13–22°N)

4. Daily bimodal ISO index from 1979 to 2017 developed by Kikuchi *et al.* (2012) (https://iprc.soest.hawaii.edu/users/kazuyosh/Bimodal_ISO.html). This bimodal index is composed of two ISO modes; the Madden-Julian Oscillation (MJO) mode, which exhibits eastward propagation during winter along the equator and the Boreal Summer ISO (BSISO) mode that exhibits northward propagation in the off-equatorial monsoon trough regions. In this study, only the BSISO mode was used. The spatio-temporal patterns of these two ISO modes are identified by applying an extended empirical orthogonal function (EEOF) analysis on the band-passed filtered daily outgoing longwave radiation data. The first two EEOF coefficients (hereafter, PC1 and PC2) are projected onto a phase-space diagram to depict the active and suppressed phases and location of the ISO. There are eight phases in this phase-space diagram and the propagation of the ISO is depicted in an anti-clockwise direction. The active convection of BSISO in Phases 1 and 2 is located over the eastern North Pacific and equatorial Indian Ocean, in Phases 2 and 3 over the Bay of Bengal, in Phases 4 and 5 over India and the maritime continent, and in Phases 6 and 7 over the western North Pacific.

2.2 | Methodology

The analysis period extends from 1979 to 2017. We only focus our analysis around Luzon Island because the monsoon break after the onset is only clear around this region, as will be shown later.

We define "Luzon Island" and its vicinity as the region within 120–122.5°E and 13–22°N. We also used the summer monsoon onset dates provided by PAGASA (Table 1). These onset dates were obtained following the criteria indicated in the 2019 memorandum of PAGASA stated as follows: (1) The beginning of a five-day period (between May and July) with total rainfall exceeds 25 mm, with three consecutive days having at least 1 mm of rainfall per day. These conditions should be satisfied in at least seven stations located over the western coast of the Philippines. These stations include: Laoag, Vigan (Sinait), Dagupan, Iba, San Jose (Mindoro), Metro Manila, Ambulong (Batangas), Iloilo, Nueva Ecija (Muñoz), Clark (Pampanga), Cubi Point (Subic), Coron (Palawan), and Cuyo (Palawan) For Metro Manila to be included in this criterion, at least three of the four Metro Manila stations (i.e., Science Garden, Sangley Point, Port Area, and Ninoy Aquino International Airport) must have satisfied (1). These stations are similar to those used by Kubota *et al.* (2017; see their Figure 1 for the location of the stations). Additionally, PAGASA has the disposition to include other variables such as prevailing westerly winds (i.e., westerly from surface to 850 hPa level) in the onset criteria. It is important to note that the summer monsoon onset date is assigned across the aforementioned stations over the western coast of the Philippines. In this study, we used the Sangley Point station as a representative of the stations over Metro Manila. We exclude Nueva Ecija (Muñoz) station in the analysis because it has a lot of missing data after 2001. In addition, we also used two additional stations that are located over the northern (Basco station) and central Luzon Island (Cabanatuan stations).

To assess the statistically significant differences in the spatial and time series plots, we used the Student's *t*-test. For the significance of the composite anomalies, we compare the composite means of the monsoon break days and their equivalent no monsoon break days in other years. For example, if a monsoon break occurred from June 11–13, 2017, then we compare the atmospheric conditions during this period to all the other June 11–13 period between 1979 and 2016 that are not classified as monsoon break periods. The analysis period for the TRMM rainfall is from 1998 to 2015, while those for the reanalysis data is from 1979 to 2017. The anomalies for the TRMM rainfall are calculated relative to the 1998–2015 mean, while those for the reanalysis data set is relative to the 1979–2017 mean. The TRMM rainfall data was only used to depict the changes in the largescale rainfall and not for the monsoon break detection.

3 | RESULTS

3.1 | Climatological characteristics of the summer monsoon over the Philippines

There are no uniform criteria in defining a monsoon break. Chen *et al.* (2004), for example, defined the monsoon break over East Asia as the period when the frontal activity diminishes and rainfall decreases to below 5 mm·day^{-1}. On the other hand, Rajeevan *et al.* (2010) defined the monsoon break during the summer monsoon over India as the period when the standardized daily rainfall anomaly is below −1 standard deviation for at least three consecutive days. In this study, we define a monsoon break as the period following the onset when rainfall decreases below 5 mm·day^{-1} and should last for at least three consecutive days. In addition, we only selected the stations with at least one break within 40 days after the onset. Hence, we came up with six stations that include Basco, Vigan, Laoag, Cabanatuan, Clark and Sangley Point that are in the central and northern Luzon Island. These stations were also selected because they have clear

decreases in rainfall several days after the onset (not shown). The 5 mm·day^{-1} value is based on Moron *et al.* (2009) who noted that the dry season over the western coast of the Philippines usually have rainfall amounts that is less than this value. It is also worth mentioning the we did not see a clear monsoon break in the stations located to the south of Luzon Island, indicating that it is only confined to the central and northern Luzon Island. Since the onset dates are assigned across the stations located over the western coast of the Philippines, we identified the breaks from the average daily rainfall from the six selected stations. We only focus on the first break following the onset in each year. The detected first post-onset breaks are summarized in Table 1. The average of the PAGASA onset dates from 1979–2017 is May 27, with standard deviation of about 15 days, while the average starting date of the monsoon break period is June 8, with standard deviation of about 17 days. On average, the first monsoon break following the onset only lasts for about 6 days and occurs 12 days after the onset. The earliest monsoon break occurred in 1984 (May 7–17), while the latest occurred in 2015 (July 19–21).

Based on the detected monsoon break periods in Table 1, we illustrate the composites of daily rainfall relative to the monsoon break period for the six PAGASA stations and TRMM rainfall averaged over Luzon Island (120–122.5°E, 13–22°N) in Figure 2. To avoid the bias from the ocean grid points, we derived the time series for the TRMM data based on the grid points over land only. Before the monsoon break period, rainfall in all the stations increases to as much as 38 mm·day^{-1}, except for Laoag station, where the rainfall first peaks at Lag −14 and exceeds 50 mm·day^{-1}. This location frequently experiences heavy rainfall events associated with shearlines (Olaguera and Matsumoto, 2020). During the monsoon break period, the rainfall drops below 5 mm·day^{-1} in all the stations and increases again to about 10 mm·day^{-1} after Lag +6. The TRMM rainfall was able to capture the mean distribution of rainfall across the six stations although the rainfall around the monsoon break period only decreased to below 5 mm·day^{-1} between Lag +2 and Lag +5. The TRMM rainfall also underestimated the rainfall between Lag −13 and Lag −4 and the peak around Lag −15. These results suggest that the TRMM rainfall can be used for depicting the spatial patterns of rainfall in this study but not for determining the timing of the monsoon break periods.

3.2 | Changes in the large-scale conditions

To further examine the development of the first post-onset break, we performed lag composite analysis, where Lag 0 corresponds to the first day of the monsoon break period. The previous and succeeding lag days are denoted with a "-" and "+" signs, respectively. Figure 3 shows the lag composites of the mean TRMM rainfall, 850 hPa winds ($WINDS_{850hPa}$), and 850 hPa *HGT* (HGT_{850hPa}), while Figure 5 shows the lag composites of the mean 200 hPa winds ($WINDS_{200hPa}$) and *HGT* (HGT_{200hPa}). Their corresponding composite anomalies are shown in Figures 4 and 6, respectively.

Based on the composite means (Figure 3a), rainfall of about 5–10 mm·day^{-1} and southeasterly $WINDS_{850hPa}$ associated with the WNPSH are apparent over the country at Lag −20. Westerly to southwesterly $WINDS_{850hPa}$ can be seen between 60–110°E and to the south of 20°N, indicating enhancement of monsoon southwesterlies in this region. The composite anomalies in Figure 4a show that easterly to northeasterly $WINDS_{850hPa}$ are apparent over the Philippines, indicating no monsoon southwesterlies intrusion over the country. The significant southwesterly $WINDS_{850hPa}$ are more remarkable over the southern tip of the Indian Subcontinent, where an anomalous cyclonic circulation can also be seen (Figure 4a). Also note from the mean composites that the western rim of the WNPSH, indicated by 1,500 m contour line, is located around 115°E on this lag day, where the southeasterly $WINDS_{850hPa}$ also converge with the southwesterly $WINDS_{850hPa}$ (Figure 3a). Prior to this day, the western rim of the WNPSH is located over the Indochina Peninsula and progressed eastward after Lag −20 (not shown). This eastward retreat of the WNPSH is a well-known feature of the ASM onset (Lau and Yang, 1997; Zhang *et al.*, 2004; Akasaka, 2010). In addition, strong southwesterly $WINDS_{850hPa}$ are apparent over the western Indochina Peninsula that is accompanied by enhanced rainfall of about 20 mm·day^{-1} based on the mean composite map in Figure 3a. Matsumoto (1997) first noted that the earliest onset of the ASM starts over the Indochina Peninsula. Zhang *et al.* (2004) later suggested that this is due to the convergence of southwesterly $WINDS_{850hPa}$ originating from the Bay of Bengal and southeasterly $WINDS_{850hPa}$ from the southern flank of the WNPSH. They also pointed out that the onset is accompanied by the reversal of meridional temperature gradient in the entire troposphere and the establishment of an easterly vertical wind shear over the Indochina Peninsula, as indicated by the anticyclonic circulation (South Asian Anticyclone; SAA) of $WINDS_{200hPa}$ centred at 105°E, 15°N (Figure 5a). The rainfall over the Indian Subcontinent is less than 5 mm·day^{-1} (Figure 3a) indicating that the summer monsoon has not started yet in this region. Moreover, enhanced rainfall can also be seen over South China and the

TABLE 1 Summary of the onset pentads, first post-onset breaks, their duration (days), and timing (days) relative to the onset dates from 1979 to 2017.

Year	Onset pentad	First post-onset break	Duration of break	Number of days relative to the onset
1979	May 11–15	May 24–26	3	13
1980	June 29–July 3	July 11–15	5	12
1981	June 4–8	June 21–29	9	17
1982	June 22–26	July 16–21	6	24
1983	June 2–6	June 9–16	8	7
1984	May 2–6	May 7–17	11	5
1985	June 5–9	July 7–10	4	32
1986	May 13–17	May 18–20	3	5
1987	June 7–11	June 17–22	6	10
1988	May 24–28	June 6–10	5	13
1989	May 14–18	May 21–25	5	7
1990	May 19–23	June 7–9	3	19
1991	June 12–16	June 25–30	6	13
1992	May 27–31	June 3–9	7	7
1993	June 23–27	June 27–July 2	6	4
1994	June 1–5	June 7–11	5	6
1995	May 12–16	May 17–20	4	5
1996	June 23–27	June 27–July 2	6	4
1997	May 21–25	June 5–15	11	15
1998	May 23–27	June 7–13	7	15
1999	June 1–5	June 7–13	7	6
2000	May 10–14	May 26–June 3	9	16
2001	May 7–11	May 16–18	3	9
2002	May 23–27	June 11–20	10	19
2003	May 22–26	June 6–13	8	15
2004	May 15–19	May 27–31	5	12
2005	May 28–June 1	June 12–14	3	15
2006	June 11–15	June 19–24	6	8
2007	May 25–29	May 30–June 1	3	5
2008	May 11–15	June 4–11	8	24
2009	May 3–7	May 10–18	9	7
2010	June 1–5	June 14–18	5	13
2011	May 23–27	May 30-June 2	4	7
2012	May 29–June 2	June 4–7	4	6
2013	June 8–12	June 23–26	4	15
2014	June 7–11	June 13–16	4	6
2015	June 17–21	July 19–21	3	32
2016	May 21–25	May 26–28	3	4
2017	May 25–29	June 11–14	4	16
Average	May 27	June 8	6	12

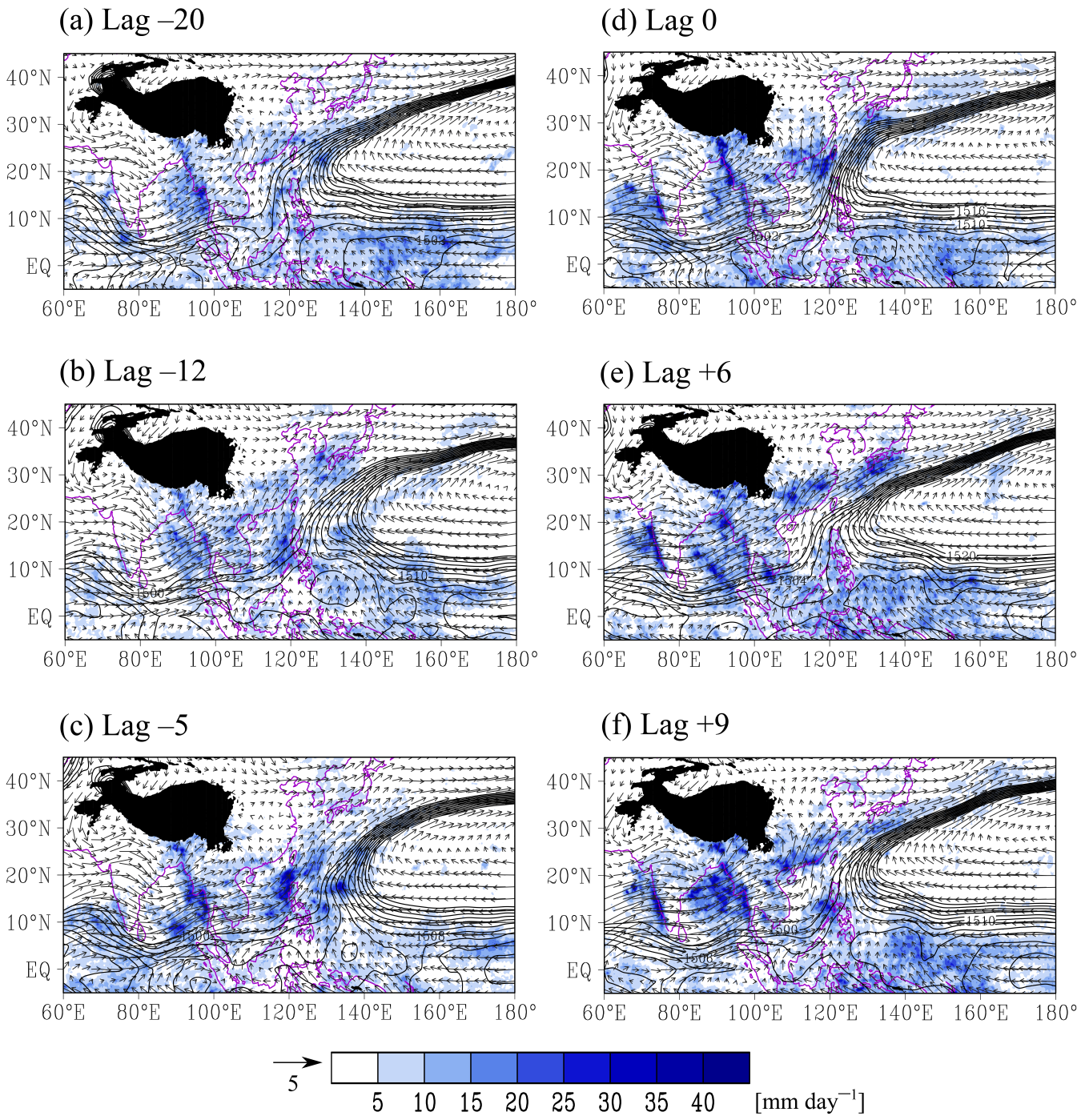

FIGURE 3 Composite means of TRMM rainfall (mm·day^{-1}; shaded), 850 hPa *HGT* (HGT_{850hPa}; m; contours), and 850 hPa winds ($WINDS_{850hPa}$; m·s^{-1}; vectors) for (a) Lag −20, (b) Lag −12, (c) Lag −5, (d) Lag 0, (e) Lag +6, and (f) Lag +9. The scale of the wind vectors is 5 m·s^{-1}. The contour interval of the HGT_{850hPa} is 2 m between 1,500 and 1,520 m. The TRMM composites are based on the 1998–2015 mean, while the $WINDS_{850hPa}$ and HGT_{850hPa} are based on the 1979–2017 mean

Okinawa region in Figure 4a, which may indicate the onset of the Mei-yu over this region.

Figures 3b and 4b show the spatial structures of the composite means and anomalies of TRMM rainfall, $WINDS_{850hPa}$, HGT_{850hPa} at Lag −12, respectively. On average, this period corresponds to the summer monsoon onset in the Philippines. Based on the mean composites in Figure 3b, the TRMM rainfall increased to about 20 mm·day^{-1}, while the western edge of the WNPSH is located around 125°E. This increase in rainfall amount is statistically significant based on the composite anomalies in Figure 4b. The southwesterly $WINDS_{850hPa}$ start to

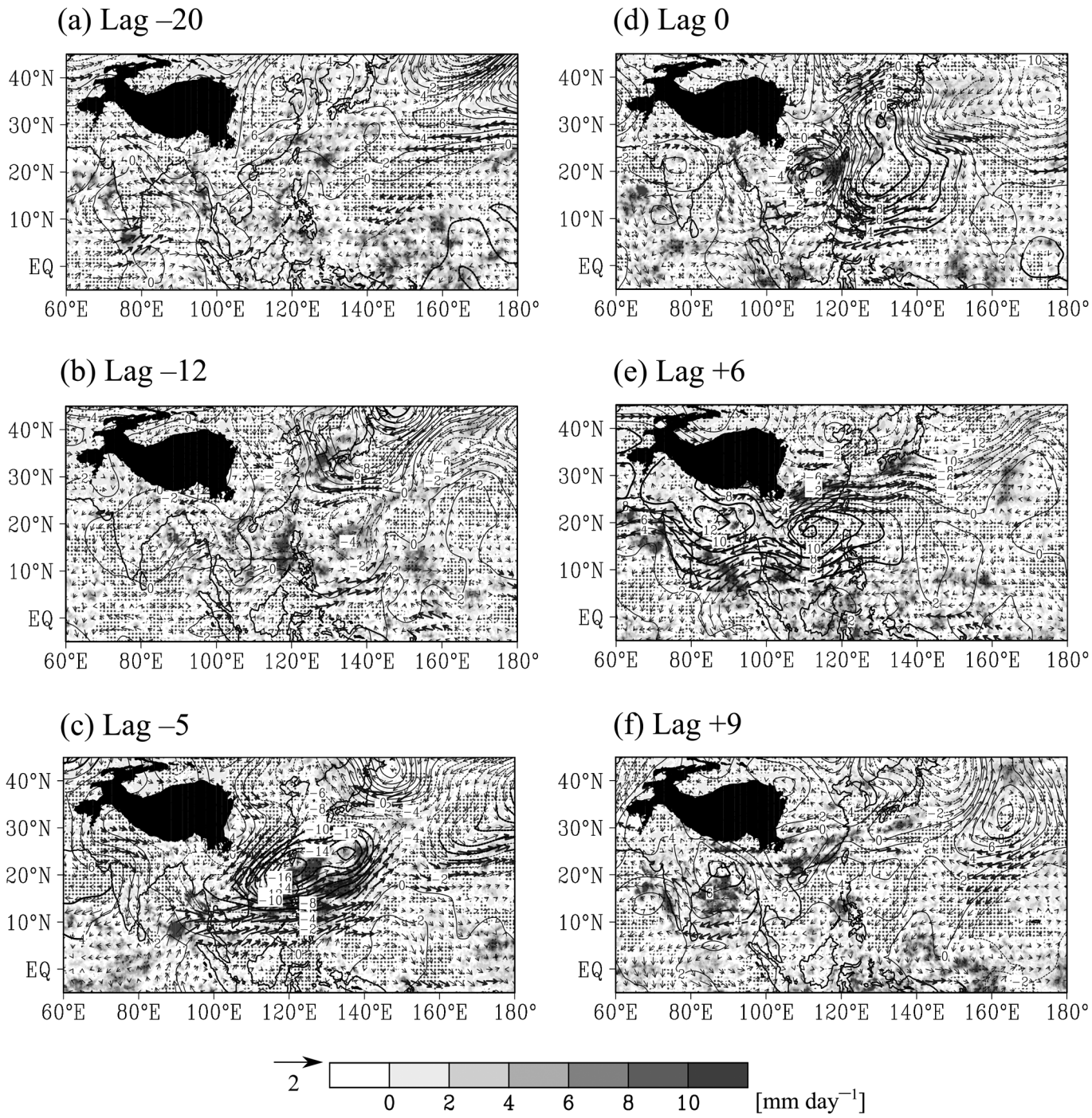

FIGURE 4 As in Figure 3 but for the composite anomalies of the TRMM rainfall (mm·day^{-1}; shaded), 850 hPa *HGT* (HGT_{850hPa}; m; contours), and 850 hPa winds ($WINDS_{850hPa}$; m·s^{-1}; vectors). The scale of the wind vectors is 2 m·s^{-1}. The contour interval of the HGT_{850hPa} is 2 m. Stippled areas, bold vectors, and thicker contours indicate statistical significance at the 95% confidence level

strengthen and stretch from the western Indochina Peninsula, SCS, Luzon Island, and the Okinawa region (Figure 4b). The rainfall over the Okinawa region further intensify during this period (Figure 4b). Also note the significant westerly $WINDS_{850hPa}$ to the south of the Philippines, which may indicate the strengthening of the ITCZ, and the presence of cross-equatorial wind flow from the Southern Hemisphere towards Mindanao-Palawan area. Westerlies can also be depicted to the west of the Indian Subcontinent based on the mean composites in Figure 3b but the rainfall is still around 5 mm·day^{-1} over this region, except on the southwest coast. At 200 hPa

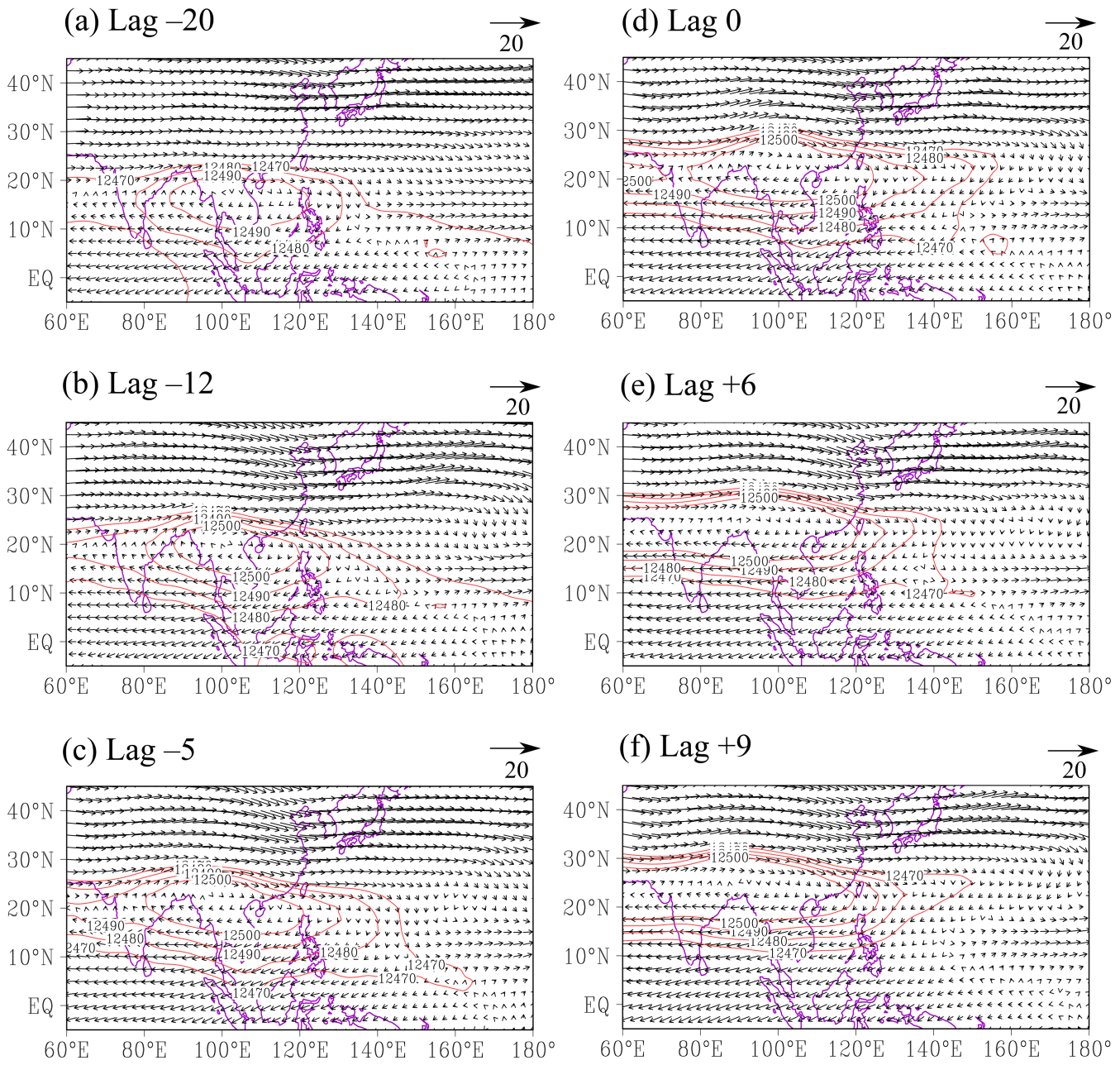

FIGURE 5 Composite means of 200 hPa WINDS ($WINDS_{200hPa}$, m s^{-1}; vectors) and 200 hPa *HGT* (HGT_{200hPa}; m; contours) for (a) lag −20, (b) lag −12, (c) lag −5, (d) lag 0, (e) lag +6, and (f) lag +9. The scale of the wind vectors is 20 m s^{-1}. The contour interval of the HGT_{200hPa} is 10 m between 12,470 and 12,500 m. the HGT_{200hPa} composites are based on the 1979–2017 mean

(Figure 5b), the SAA intensifies and progresses northwestward. Northeasterly $WINDS_{200hPa}$ appear over the SCS and southern Luzon Island (Figure 5b). This intensification of the SAA has been linked by previous studies to the increase in the diabatic heating following the abrupt expansion of warm air over the Tibetan Plateau (e.g., Yanai *et al*., 1992). Yanai *et al*. (1992) suggested that such warming leads to the reversal of the meridional temperature gradient over the south of the Tibetan Plateau that is favourable for the quick establishment of the southwesterly $WINDS_{850hPa}$ over the tropical Indian Ocean. The HGT_{200hPa}, on the other hand, increased significantly over the eastern Indochina Peninsula and central SCS (Figure 6b).

At Lag −5 (Figure 3c), the WNPSH further retreats eastward (near 135°E), westerly to southwesterly $WINDS_{850hPa}$ are established, and rainfall increases along the equator and 10°N. Enhanced rainfall (~10 mm·day^{-1}) can also be seen over the southwestern Indian Subcontinent and SCS, while those over Luzon Island increases to

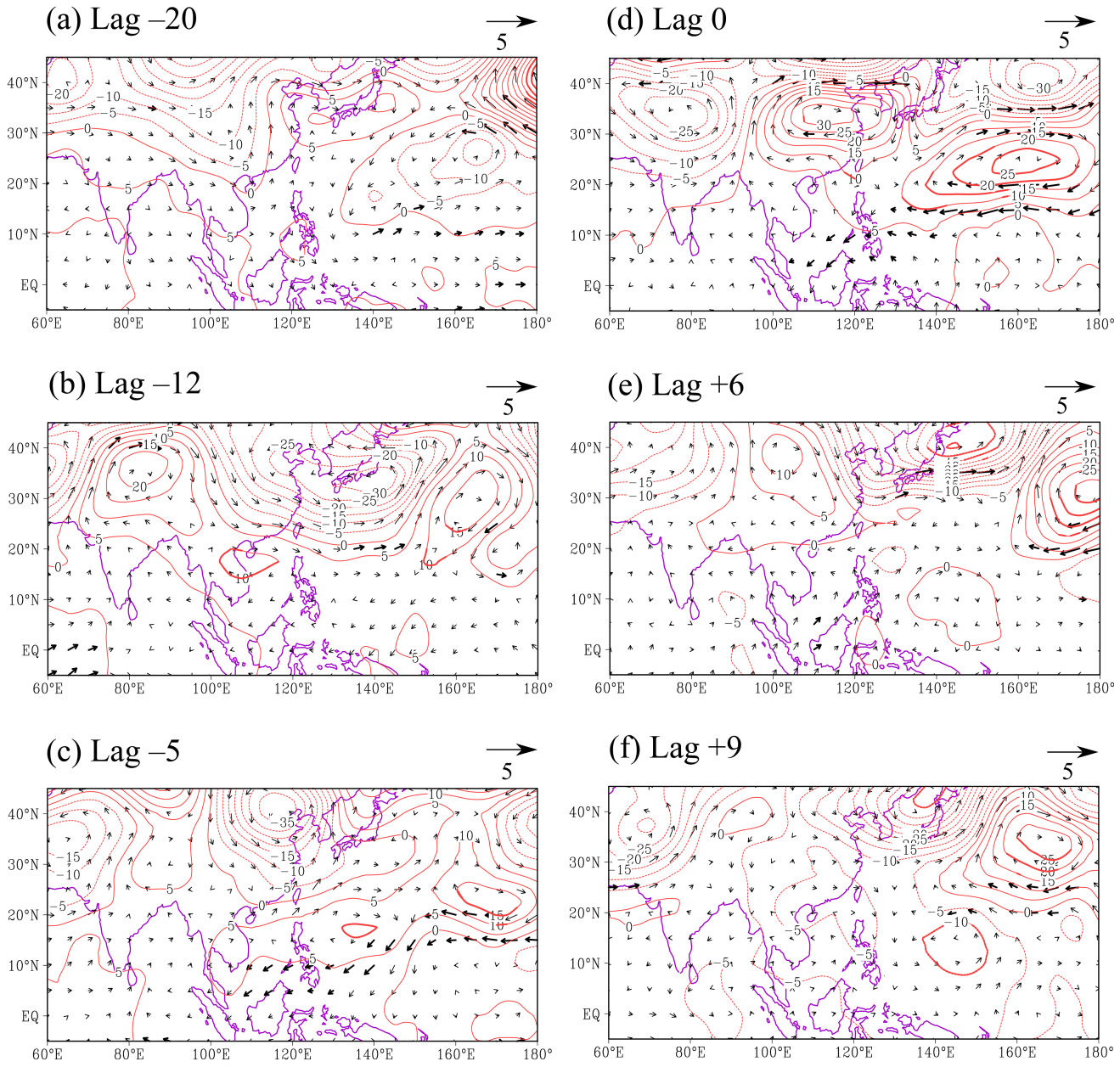

FIGURE 6 As in Figure 5 but for the composite anomalies of 200 hPa winds ($WINDS_{200hPa}$; m s^{-1}; vectors) and 200 hPa HGT (HGT_{200hPa}). The contour interval is 5 m, while the scale of the vectors is 10 m s^{-1}. Bold vectors and thicker contours indicate statistical significance at the 95% confidence level

about 35 mm·day^{-1} (Figure 3c). Significant changes in rainfall, $WINDS_{850hPa}$, and HGT_{850hPa} are apparent between 100–150°E and 5–30°N (Figure 4c). At 200 hPa (Figure 5c), the eastern edge of the SAA is located around 160°E. Northeasterly $WINDS_{200hPa}$ along the eastern edge of this anticyclone can be seen over the central Luzon Island. As for the composite anomalies in Figure 6c, significant easterly $WINDS_{200hPa}$ can be seen over the southern Philippines (south of 10°N) as part of the anomalous upper level anticyclonic circulation, centred around 135°E. These significant changes correspond with the anomalous low-level cyclonic circulation and westerly $WINDS_{850hPa}$ over this region (Figure 4c).

At Lag 0 (Figure 3d), the WNPSH moves westward and the western edge of the 1,500 m HGT_{850hPa} contour line is located over Luzon Island based on the composite means. Rainfall also decreases to 5 mm·day^{-1} over Luzon Island. This implies that the monsoon break is a significant event after the onset (Figure 3(d)). Enhanced westerly $WINDS_{850hPa}$ can be seen over the western Indian Subcontinent (Figure 3(d)) that is associated with the southward shift of the 1,500 m HGT_{850hPa} contour line,

and the rainfall over this region reaches by about 25 mm·day^{-1}. This is consistent with the onset of the Indian summer monsoon. On the other hand, the northern part of the WNPSH establishes the Mei-yu/Baiu frontal zone over South China, Taiwan, and the Okinawa region, as indicated by the enhanced rainfall in these regions (Figure 3d). The anomalous cyclonic circulation depicted in Figure 4d) over the WNP weakens, which is now centred around 115°E, 20°N. An anomalous anticyclonic circulation centred around 130°E, 20°N affects the Philippines, which is accompanied by a significant decrease in rainfall. This anomalous anticyclonic circulation extends up to 40°N over the Korean Peninsula and 140°E over the western North Pacific. At 200 hPa (Figure 5d), the SAA moves further northwest of the Indochina Peninsula and its centre is located around 100°E, 22°N based on the mean composites. Easterly/northeasterly $WINDS_{200hPa}$ can be seen over the Philippines during this period. The significant changes in the $WINDS_{200hPa}$ are located to the south and east of the Philippines during this period (Figure 6(d)). In fact, the $WINDS_{200hPa}$ are relatively weaker around the country. Two anomalous anticyclonic circulations can be seen along 30–40°N over East Asia and 15–30°N over the northern Pacific. The change in the HGT_{200hPa} is more significant in the latter region (Figure 6d).

At Lag +6 (Figures 3e and 4e), the western edge of the HGT_{850hPa} contour line is still located over Luzon Island and rainfall over this region is relatively weaker compared to those over the western Indian Subcontinent, western Indochina Peninsula, and Okinawa region (Figure 3e). Based on the composite anomalies (Figure 4e), an anomalous anticyclonic circulation is centred around the northern SCS, which is accompanied by a decrease in rainfall in the same region including the northern Philippines. Significant easterly $WINDS_{850hPa}$ change can be depicted along 10–20°N over the northern Indian Subcontinent, Indochina Peninsula and central Philippines, which may indicate a weakening of the monsoon southwesterlies. In addition, significant westerly $WINDS_{850hPa}$ can be depicted over mainland China and the southwest Japan region that are accompanied by significant increases in rainfall amounts. Another remarkable feature is the convergence of the monsoon westerlies with the southeasterlies along the southern flank of the WNPSH near the equatorial region around 120°E based on the mean composites in Figure 3(e). This indicates the strengthening of the ITCZ. At 200 hPa, the SAA expands westward, and progresses further north (Figure 5e). Its northern edge is located along 30°N.

At Lag +9 (Figure 3f and 4f), the western edge of the HGT_{850hPa} shifts eastward and rainfall starts to increase again to about 20 mm·day^{-1} over Luzon Island based on the mean composites. Also note the significant increases in rainfall amounts over the western Indian Subcontinent, Bay of Bengal, Southern China, and south of mainland Japan. At 200 hPa (Figure 5(f)), the SAA continues its northwestward advance.

In the succeeding lag days, we found that the WNPSH progresses northwards and rainfall amounts start to increase over mainland Japan, indicating the start of the Baiu season over there (not shown). How does the westward propagation of WNPSH induce dry weather conditions over Luzon Island? To answer this question, we also looked at the lag composites of 500 hPa vertical velocity, which can also reflect the changes in the rainfall. At Lag 0, significant descending vertical velocity anomalies were found over Luzon Island (not shown), which corroborates the presence of the anomalous anticyclonic circulation over this region. In general, the westward intrusion of the WNPSH induces mid-tropospheric descent over Luzon Island. Olaguera *et al.* (2018a) noted that such mid-tropospheric descent is one of the factors that induces unfavourable conditions for rainfall over Luzon Island.

3.3 | Characteristics of the monsoon break period

Moisture transported by the monsoon westerlies is essential for the summer monsoon rainfall of the Philippines (e.g., Flores and Balagot, 1969; Olaguera *et al.*, 2018a). Therefore, we also examined the time series of the averaged vertically integrated moisture flux convergence (*VIMFC*) over Luzon Island (120–122.5°E, 13–22°N), as shown in Figure 7(a). It is worth mentioning that although this is a small region, we found that the time series of the *VIMFC*, *U*, *V*, and *HGT* are not sensitive to the averaging location. That is, when we extended the longitudinal boundaries to 117.5–125°E, we found that the resulting distributions are similar to those found using the smaller region (not shown). The vertical integration was performed from 1,000 to 300 hPa following Olaguera *et al.* (2018a, 2018b). The *VIMFC* reaches by about 12×10^{-5} kg m^{-2} s^{-1} from Lag −12 to Lag −1 and decreases during the break period (i.e., Lag +1 to Lag +6), indicating enhanced convergence and divergence before and during the monsoon break period, respectively. In the succeeding lag days, convergence reappears over Luzon Island (between Lag +6 to Lag +20). However, the values are weaker (around 4×10^{-5} kg m^{-2} s^{-1}) compared to those before the monsoon break period. This weaker *VIMFC* is consistent with lower rainfall values after the monsoon break period, as shown in Figure 2.

Also shown in Figure 7a is the averaged zonal wind at 850 hPa (U_{850hPa}) over Luzon Island. It appears that

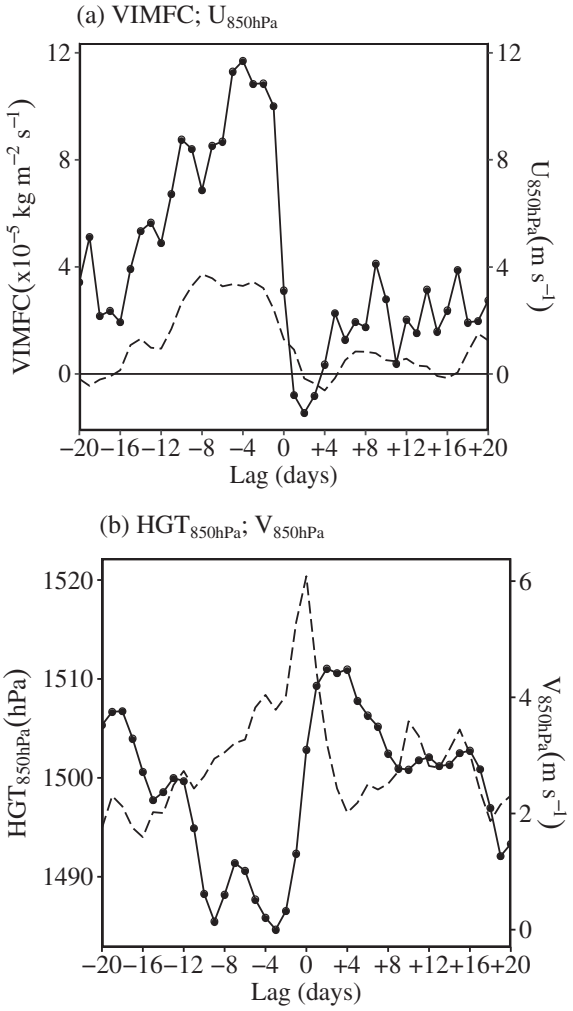

FIGURE 7 Time series of (a) vertically integrated moisture flux convergence (*VIMFC*; solid line; $\times 10^{-5}$ kg m^{-2} s^{-1}) and zonal wind at 850 hPa (U_{850hPa}; dashed line; m s^{-1}) over Luzon Island (120–122.5°E, 13–22°N). (b) As in (a) but for the geopotential height (HGT_{850hPa}; solid line; m) and meridional wind at 850 hPa (V_{850hPa}; dashed line; m s^{-1}). The solid horizontal line in (a) indicates the 0 *VIMFC* and U_{850hPa}

the enhanced *VIMFC* before the monsoon break period is accompanied by enhanced westerly U_{850hPa}, while during the break period, the westerly U_{850hPa}, weakens and easterlies appear over Luzon Island until Lag +6. Such easterly U_{850hPa} after the summer monsoon onset over the Philippines was also noted by the pentad-based climatological field in Matsumoto *et al.* (2020; see their Figure 4). In the succeeding lag days, the U_{850hPa} remained around +2 m·s^{-1}, which is relatively weaker compared to the days before the monsoon break period. It can also be seen in Figure 3d,e that south to southeasterly $WINDS_{850hPa}$ are apparent over Luzon Island during the monsoon break period. The meridional wind component at 850 hPa (V_{850hPa}) averaged over Luzon Island is shown in Figure 7b. The V_{850hPa} exceeds 2 m·s^{-1} after Lag −12 and reaches its peak magnitude (6 m·s^{-1}) at Lag 0. Afterwards, it abruptly decreases to 2 m·s^{-1} to Lag +4 and increase again to 3 m·s^{-1} after Lag +8.

To explain why such weakening of the *VIMFC* persisted, we checked the averaged HGT_{850hPa} over Luzon Island in Figure 7b. Between Lag −12 and Lag −1, the WNPSH decreases below 1,490 m, which is consistent with Figure 4b, where the WNPSH is located to the east of the Philippines. During the break period, the HGT_{850hPa} increases to about 1,512 m, which is also consistent with the westward intrusion of the WNPSH, as shown in Figure 4d,e. From Lag +7 to Lag +12, the values of the HGT_{850hPa} remained below 1,500 m but not as remarkable compared to those during the onset period. This means that the WNPSH is still located near Luzon Island and has not progressed northwards yet. This may have hindered the intrusion of westerly $WINDS_{850hPa}$ over Luzon Island, which is also consistent with the easterly $WINDS_{850hPa}$ anomalies in the same region shown in Figure 3.

Wu and Wang (2001) found that the summer monsoon over the WNP (WNPSM; 110–160°E, 10–20°N) undergoes three distinct stages. They noted that the first stage of abrupt rainfall enhancement occurs around pentad 27–28 (May 11–20) over the SCS. The second stage occurs around P34 (June 15–19) in the southwestern Philippine sea, and the third stage occurs around pentad 40–41 (July 15–24) to the northeast of the Philippines. The onset of the rainy season over Luzon Island coincides with the first stage of the WNPSM, while the monsoon break (June 8–14) over Luzon Island occurs during the transition pentads (pentad 32–33) between the first and second stages of the WNPSM. Wu and Wang (2001) showed that between pentads 32 and 33, the monsoon trough, defined as the convergence zone of the monsoon westerly wind and easterly trade wind, is located across the Philippines (see their Figure 3b). After these pentads, the monsoon trough shifts northeastwards. Therefore, the reappearance of westerly U_{850hPa} and enhancement of *VIMFC*, as shown in Figure 7a, after the monsoon break period is related to the northeastward shift of the monsoon trough and enhancement of rainfall over the WNP.

3.4 | Possible mechanisms inducing the monsoon break

Ueda and Yasunari (1996) pointed out the importance of ISOs as triggers for the northeastward advance of the summer monsoon rainfall from the SCS to the east Philippine Sea. In general, the ISO during boreal summer exhibits northward propagation (BSISO mode), while

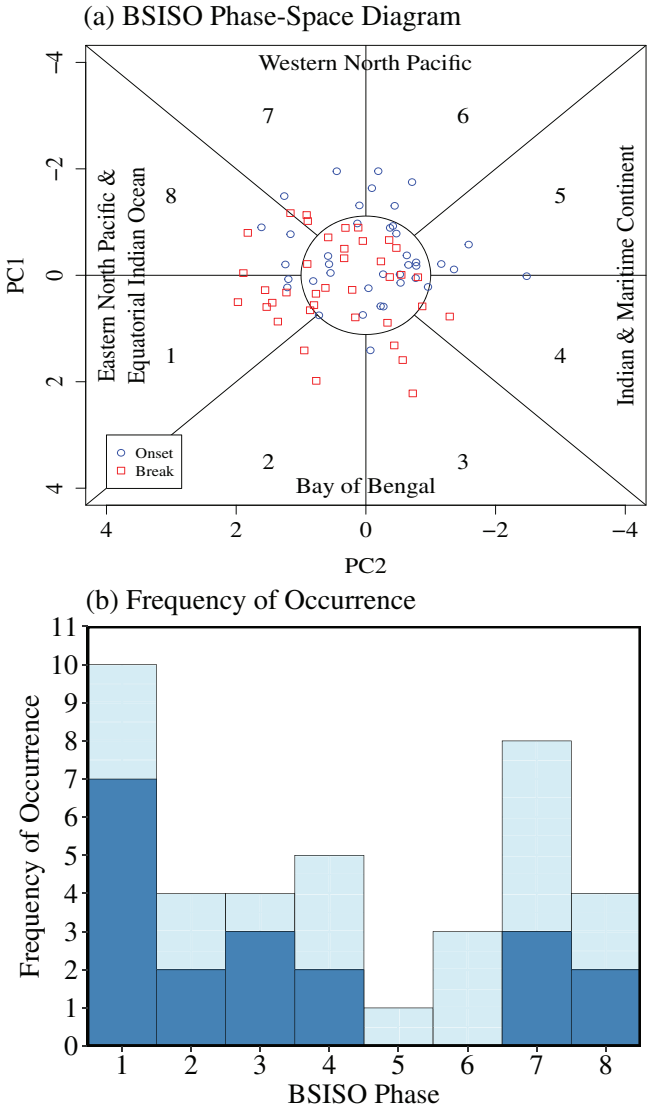

FIGURE 8 (a) Phase-space diagram of the boreal summer intraseasonal oscillation (BSISO) mode for the onset and break (first day) periods. (b) Frequency of occurrence of the monsoon break in each BSISO phase. The vertical (horizontal) axis in (a) represents the PC1 (PC2) of the BSISO. The inner circle in (a) indicates one standard deviation, while the dividing lines indicate the location of the different BSISO phases. Light shadings in (b) indicate total counts in each phase, while dark shadings indicate counts above one standard deviation in each phase

during boreal winter it exhibits eastward propagation (MJO mode) (Madden and Julian, 1971; Fukutomi and Yasunari, 1999, 2002; Kajikawa and Yasunari, 2005; Kikuchi and Wang, 2010; Kikuchi *et al.*, 2012). Kikuchi *et al.* (2012) developed a bimodal index to determine the location of these two ISO modes at any time of the year. It is surprising that the composites of rainfall as shown in Figure 3 resemble the pattern of the BSISO mode in Kikuchi *et al.* (2012) (see their Figure 8b). As depicted in Figure 3, the rainfall starts to increase first around the Bay of Bengal-Indochina Peninsula area (Figure 3a), then expands to the SCS-west Philippines (Figure 3b,c), and to the Okinawa region (Figure 3d,e). This is accompanied by the westward and northward migration of the WNPSH. This suggests that the active-break cycle of rainfall in the early summer monsoon season of the Philippines is modulated by the phase change of the BSISO. To assess this issue, we constructed a phase-space diagram, as shown in Figure 8a, to depict the relationship among the BSISO, onset, and break periods (i.e., the first day of both the onset and the break periods). Most of the onset dates are classified in Phases 5, 6, 7, and 8, when the active convection of the BSISO mode is apparent over the WNP (figure 8b of Kikuchi *et al.*, 2012). On the other hand, most of the break dates are classified in Phases 1, 2, 3, and 4, when the suppressed convection of the BSISO mode is apparent over the WNP. This suppressed convection favours the westward/southward expansion of the WNPSH (e.g., Huang and Sun, 1992).

Figure 8b shows the frequency of occurrence of the monsoon break in the eight phases of the BSISO mode. The darker shadings indicate strong BSISO phases. There are 10 monsoon break cases during Phase 1, 7 of which are associated with strong suppressed phase of the BSISO mode. There are no strong cases that were observed in Phases 5 and 6, while almost half of the cases in Phases 7 and 8 are strong. In total, about 23 cases occurred between Phases 1 and 4, 14 cases of which, have amplitudes exceeding one standard deviation. These results suggest that the phase of the BSISO can modulate the frequency of occurrence of the monsoon break over Luzon Island, with the strongest relationship found during Phase 1 of the BSISO mode.

To test the significance of the probability of occurrence of the monsoon break between Phases 1 and 4, we performed a Monte Carlo simulation, which is described as follows. For this test, we used the average daily rainfall across the six PAGASA stations from 1979 to 2017. We only used the days from the last day of the monsoon onset pentad since PAGASA defines the onset as the start of a 5-day period to the last day of the monsoon break period in each year. For example, the onset pentad in year 1979 is May 11–15, while the break period is May 24–26. Then, the rainfall data from May 16 to May 26 in this year were used for the Monte Carlo simulation. We provided the list of onset pentads from 1979 to 2017 in Table 1. We pooled all the days following the above condition from 1979 to 2017. The observed statistics are those depicted in Figure 8b, with a total of 23 monsoon break cases between Phases 1 and 4 from 1979 to 2017. The null hypothesis for this test is that this count occurred randomly by chance. We resampled the pooled data with

replacement for 100,000 times (i.e., 100,000 simulations), while preserving the phases in each day. Then, we counted the frequency of occurrence of the monsoon break from each simulation. The resultant probability distribution for the frequency of occurrence of the monsoon break from the randomized 39-year pooled data is shown in Figure S1. The result indicates that the probability of occurrence for more than 23 monsoon break cases is less than 5%. Therefore, taking a 95% confidence level, we reject that null hypothesis, which implies that the occurrence of the monsoon break is statistically significant.

4 | DISCUSSION

We found that about 59% (23/39) of the monsoon breaks are associated with the suppressed phases of the BSISO mode over the WNP, with the strongest relationship occurring during Phase 1. An anomalous anticyclonic circulation appears over the WNP during the suppressed phases of the BSISO, which leads to suppressed convection in this region. Huang and Sun (1992) suggested that this suppressed convection over the WNP leads to the strengthening and southwestward shift of the WNPSH. In this study, we found that the westward expansion of the WNPSH during the monsoon break period induced enhanced divergence, mid-tropospheric descent, weakening of the monsoon westerlies, and subsequent decrease in moisture transport over Luzon Island. After the monsoon break period, weaker moisture convergence and monsoon westerlies were still apparent over Luzon Island compared to those during the onset period. The weaker monsoon westerlies can be explained by the fact that the WNPSH is still in the vicinity of Luzon Island, which could have hindered the intrusion of the westerly winds over this region, and that it has not progressed northwards yet. The time-series of the HGT_{850hPa} shows that its magnitude remained between 1,500 and 1,512 m even after the break period compared to those during the onset period, when it decreased to about 1,485 m. We also found that most of the onset dates coincided with the active phases of the BSISO (i.e., Phases 5–8). An anomalous cyclonic circulation appears over the WNP during these phases, which favours the enhancement of rainfall

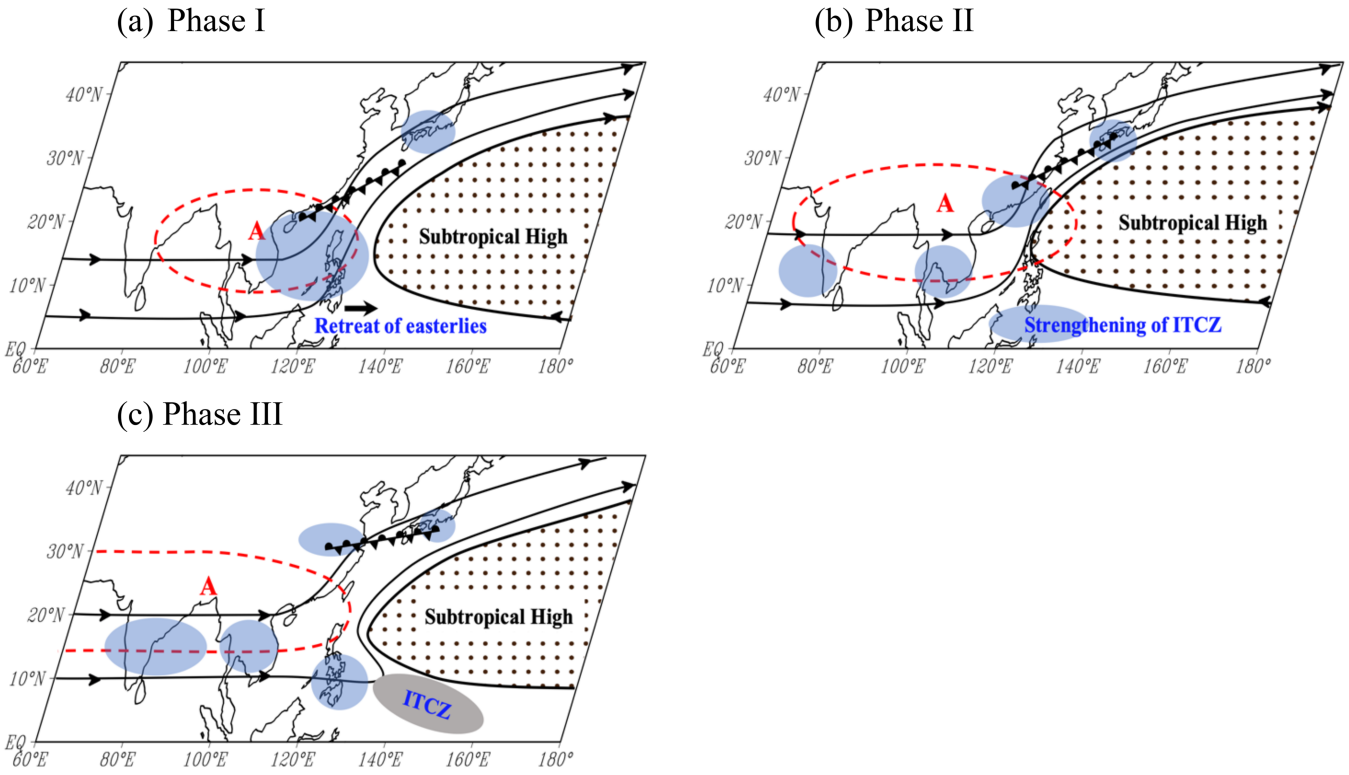

FIGURE 9 Schematic diagram illustrating the three-phase onset process of the summer monsoon over the Philippines: (a) phase I (onset phase; mid to late May), (b) phase II (break phase; early June), (c) phase III (monsoon revival phase; mid-June). Phases I, II, and III correspond to the periods between Lag −12 and Lag −1, Lag 0 to Lag +6, Lag +7 to Lag +20, in Figures 3, 4, 5, 6, and S2, respectively. The red broken line and "A" indicates the location of the anticyclonic circulation at 200 hPa depicted by the 12,490-geopotential height contour line in Figure 5. Blue circles indicate the regions with significant rainfall increase based on the composite rainfall maps in Figures 3, 4, and S2

over the Philippines. Kubota *et al*. (2017) found that tropical cyclones may trigger the early summer monsoon onset over the Philippines by accelerating the moist southwesterly winds. During active phases of the BSISO, tropical cyclone activity over the WNP is enhanced (Li and Zhou, 2013), increasing the probability of early summer monsoon onset over the Philippines.

The precise controlling mechanism for the zonal displacement of the WNPSH in early summer needs further investigation. Some studies used numerical models to explain the mechanisms controlling its zonal displacement during the summer monsoon season (e.g., Lu and Dong, 2001). However, these numerical models have large uncertainties and ignores the atmosphere–ocean interactions leading to inconsistent results compared to actual observations (e.g., Wang *et al*., 2005; Kawatani *et al*., 2008; Kubota *et al*., 2016; Dado and Takahashi, 2017). Nevertheless, correctly simulating the timing of the monsoon break using numerical models is also of great interest.

5 | SUMMARY AND CONCLUSION

This study investigated the climatology of the first post-onset break in rainfall over Luzon Island (120–122.5°E, 13–22°N) from 1979 to 2017. We defined the monsoon break as the period with rainfall below 5 mm·day^{-1} after the onset, as defined by PAGASA, that lasted for at least three consecutive days. On average, the examined monsoon breaks lasted for about 6 days and occurred 12 days after the onset. The climatological onset date from 1979–2017 is May 27, while the first day of the monsoon break period is June 8.

With the appearance of a monsoon break after the onset, it can be inferred that the early stage of the summer monsoon of the Philippines can be divided into three distinct and abrupt phases, as schematically illustrated in Figure 9. We illustrate the composite means and anomalies of the largescale circulation features for each phase in Figures S2 and S3. The monsoon onset (Phase 1), break (Phase II), and revival (Phase III) phases are defined as the periods from Lag −12 to Lag −1, Lag 0 to Lag +6, and Lag +7 to Lag +20, respectively. We carefully checked the areas with statistically significant increases in rainfall amounts within each phase and only indicated them in Figure 9.

Phase I (Onset Phase; Figure 9a) features the eastward retreat of the WNPSH, the northward advance of the Tibetan/South Asian anticyclone (SAA), and the onset of the summer monsoon over the SCS and west coast of the Philippines from mid to late May. This phase almost corresponds to the period from Lag −12 to Lag −1 in Figures 3–6, and S2a, S2d, and S3a. In this phase, the centre of the SAA is located over the Indochina Peninsula. Significant rainfall increase is observed over the SCS-Philippines region and over the Okinawa region. Westerly $WINDS_{850hPa}$ are apparent over Bay of Bengal, Indochina Peninsula, and SCS, while southwesterly $WINDS_{850hPa}$ are apparent over Luzon Island to the North Pacific. The eastward retreat of the WNPSH is accompanied by the weakening of easterly $WINDS_{850hPa}$ around 140°E along 5°N. This phase is also consistent with the first stage of the WNPSM as noted by Wu and Wang (2001). They further noted that the monsoon trough is established abruptly over the eastern SCS from mid to late May.

Phase II (Break Phase; Figure 9b) features the sudden westward intrusion of the WNPSH in the lower level over Luzon Island, the northwestward migration/intensification of the SAA in the upper level, and the development of the ITCZ. This phase largely corresponds to the period between Lag 0 and Lag +6 in Figures 3–6, S2b, S2e, and S3b. In this phase, the westerly $WINDS_{850hPa}$ along 10–18°N (Figures 3 and 4) intensify. The western ridge of the WNPSH is located over Luzon Island and reduces the moisture and rainfall in this region. Significant increase in rainfall was found over the northern SCS including Taiwan. The weakening of easterlies and rainfall enhancement over the southern Philippines may indicate the development of the ITCZ. In the upper-level, the SAA moves northwestward over the northwestern part of the Indochina Peninsula. The increase in rainfall over the western Indian Subcontinent is consistent with the onset of the summer monsoon over this region. In addition, this phase corresponds to the transition period between the first and second stages of the WNPSM as noted by Wu and Wang (2001). Based on their Figure 3, the monsoon trough is located across the Philippines in this phase and progresses northeastward. Wang and Xu (1997) examined the wet and dry phases of CISO over the WNP. The monsoon break over Luzon Island in early June also coincides with a dry phase of the CISO along 15–20°N, although they noted that the peak of this dry phase is around the last week of May.

Phase III (Monsoon Revival Phase; Figure 9c) features the revival of the summer monsoon over the Philippines, further expansion of the SAA in the upper level, intensification of the ITCZ, and the mature phase of the Mei-yu/Baiu over central China and mainland Japan. This phase corresponds to the period between Lag +7 and Lag +20 in Figures 3–6, S2c, S2f, and S3c. The WNPSH shifts to the east of the Philippines. In this phase, the rainfall starts to increase again over Luzon Island. A monsoon break occurs over Taiwan, following the northward migration of the WNPSH. The intensification of the ITCZ is indicated by the significant rainfall increase to the

south and east of the Philippines as well as the westerly $WINDS_{850hPa}$ intrusion until 150°E and to the south of 15°N. In the upper level, enhanced northeasterly $WINDS_{200hPa}$ along the eastern flank of the SAA are apparent over Luzon Island, which is consistent with the enhanced $WINDS_{850hPa}$ in this region. This phase corresponds to the start of the second stage of the WNPSM as noted by Wu and Wang (2001). Based on their Figures 2 and 3, the second stage of the WNPSM is characterized by significant rainfall increase over the western Philippine Sea in mid-June, enhancement of westerly $WINDS_{850hPa}$ along 5–15°N, northeastward shift of the monsoon trough, and northward displacement of the WNPSH.

The rainfall contribution of the different rainfall-producing weather disturbances in these three phases will be examined in future studies. In addition, how the sub-seasonal variabilities in the summer monsoon season of the Philippines, in general, are influenced by ENSO is also another interesting topic for future study.

ACKNOWLEDGMENTS

The authors are grateful to Dr. Tomoshige Inoue and Prof. Fumiaki Fujibe of the Department of Geography, Tokyo Metropolitan University for their useful comments and suggestions. The authors are also grateful for the insightful comments and suggestions from the editor and anonymous reviewers in further improving this manuscript.

CONFLICT OF INTEREST

The authors declare that they have no competing interests.

ORCID

Lyndon Mark P. Olaguera https://orcid.org/0000-0002-1603-9255
Jun Matsumoto https://orcid.org/0000-0003-1551-9326
Hisayuki Kubota https://orcid.org/0000-0003-0693-1618

REFERENCES

Akasaka, I. (2010) Inter-annual variations in seasonal march of rainfall in The Philippines. *International Journal of Climatology*, 30, 1301–1314. https://doi.org/10.1002/joc.1975.

Akasaka, I., Morishima, W. and Mikami, T. (2007) Seasonal march and its spatial difference of rainfall in The Philippines. *International Journal of Climatology*, 27, 715–725. https://doi.org/10.1002/joc.1428.

Asuncion, J.F. and Jose, A.M. (1980) *A Study of the Characteristics of the Northeast and Southwest Monsoons in The Philippines*. Quezon City, Philippines: PAGASA, p. 195.

Cayanan, E.O., Chen, T., Argete, J., Ten, M. and Nilo, P. (2011) The effect of tropical cyclones on southwest monsoon rainfall in The Philippines. *Journal of the Meteorological Society of Japan*, 89, 123–139. https://doi.org/10.2151/jmsj.2011-A08.

Chen, T.C., Wang, S.Y., Huang, W.R. and Yen, M.C. (2004) Variation of the east Asian summer monsoon rainfall. *Journal of Climate*, 17, 744–762 10.1175/15200442(2004)017<0744:VOTEAS>2.0.CO;2.

Cruz, F.T., Narisma, G.T., Villafuerte, M.Q., Chua, K.C. and Olaguera, L.M. (2013) A climatological analysis of the southwest monsoon rainfall in The Philippines. *Atmospheric Research*, 122, 609–616. https://doi.org/10.1016/j.atmosres.2012.06.010.

Dado, J.M.B. and Takahashi, H.G. (2017) Potential impact of sea surface temperature on rainfall over the western Philippines. *Progress in Earth and Planetary Science*, 4, 23. https://doi.org/10.1186/s40645-017-0137-6.

Flores, J.F. and Balagot, V.F. (1969) Climate of The Philippines. In: Arakawa, H. (Ed.) *Climates of Northern and Eastern Asia, World Survey of Climatology*, Vol. 8 Amsterdam: Elsevier, pp. 159–213.

Fukutomi, Y. and Yasunari, T. (1999) 10-25-day intraseasonal variations of rainfall and circulation over East Asia and western North Pacific during early summer. *Journal of the Meteorological Society of Japan*, 77, 753–769. https://doi.org/10.2151/jmsj1965.77.3_753.

Fukutomi, Y. and Yasunari, T. (2002) Tropical-extratropical interaction associated with the 10-25-day oscillation over the western Pacific during the northern summer. *Journal of the Meteorological Society of Japan*, 80, 311–331. https://doi.org/10.2151/jmsj.80.311.

Huang, R. and Sun, F. (1992) Impacts of tropical western Pacific on the east Asian summer monsoon. *Journal of the Meteorological Society of Japan*, 70, 243–256. https://doi.org/10.2151/jmsj1965.70.1B_243.

Huffman, G.J. and Bolvin, D.T. (2018) *Real-Time TRMM Multi-Satellite Precipitation Analysis Dataset Documentation*. https://docserver.gesdisc.eosdis.nasa.gov/public/project/GPM/3B4XRT_doc_V7.pdf.

Hung, C.W. and Hsu, H.H. (2008) The first transition of the Asian summer monsoon, intraseasonal oscillation, and Taiwan Meiyu. *Journal of Climate*, 21, 1552–1568. https://doi.org/10.1175/2007JCLI1457.1.

Kajikawa, Y. and Yasunari, T. (2005) Inter-annual variability of the 10–25- and 30–60-day variation over the South China Sea during boreal summer. *Geophysical Research Letters*, 32, L04710. https://doi.org/10.1029/2004GL021836.

Kanamitsu, M., Ebisuzaki, W., Woollen, J., Wan, S.K., Hnilo, J.J., Fiorino, M. and Potter, G.L. (2002) NCEP-DOE AMIP-II reanalysis (R2). *Bulletin of the American Meteorological Society*, 83, 1631–1643. https://doi.org/10.1175/BAMS-83-11-1631.

Kawatani, Y., Ninomiya, K. and Tokioka, T. (2008) The North Pacific subtropical high characterized separately for June, July, and august: zonal displacement associated with submonthly variability. *Journal of the Meteorological Society of Japan*, 86, 505–530. https://doi.org/10.2151/jmsj.86.505.

Kikuchi, K. and Wang, B. (2010) Formation of tropical cyclones in the northern Indian Ocean associated with the two types of tropical intraseasonal oscillation modes. *Journal of the Meteorological Society of Japan*, 88, 475–496. https://doi.org/10.2151/jmsj.2010-313.

Kikuchi, K., Wang, B. and Kajikawa, Y. (2012) Bimodal representation of tropical intraseasonal oscillation. *Climate Dynamics*, 38, 1989–2000. https://doi.org/10.1007/s00382-011-1159-1.

Kubota, H., Kosaka, Y. and Xie, S.P. (2016) A 117-year long index of the Pacific-Japan pattern with application to interdecadal variability. *International Journal of Climatology*, 36, 1575–1589. https://doi.org/10.1002/joc.4441.

Kubota, H., Shirooka, R., Matsumoto, J., Cayanan, E.O. and Hilario, F.D. (2017) Tropical cyclone influence on the long-term variability of The Philippines summer monsoon onset. *Progress in Earth and Planetary Science*, 4, 27. https://doi.org/10.1186/s40645-017-0138-5.

Lau, K.M., Yang, G.J. and Shen, S.H. (1988) Seasonal and intraseasonal climatology of summer monsoon rainfall over East Asia. *Monthly Weather Review*, 116, 18–37. https://doi.org/10.1175/1520–0493(1988)116<0018:SAICOS>2.0.CO;2.

Lau, K.M. and Yang, S. (1997) Climatology and inter-annual variability of the southeast Asian summer monsoon. *Advances in Atmospheric Sciences*, 14, 141–162. https://doi.org/10.1007/s00376-997-0016-y.

Li, R.C.Y. and Zhou, W. (2013) Modulation of western North Pacific tropical cyclone activity by the ISO. Part II: tracks and landfall. *Journal of Climate*, 26, 2919–2930. https://doi.org/10.1175/JCLI-D-12-00211.1.

LinHo and Wang, B. (2002) The time-space structure of the Asian-Pacific summer monsoon: a fast annual cycle view. *Journal of Climate*, 15, 2001–2019. https://doi.org/10.1175/1520-0442(2002)015<2001:TTSSOT>2.0.CO;2.

Lu, R. and Dong, B. (2001) Westward extension of the North Pacific subtropical high in summer. *Journal of the Meteorological Society of Japan*, 79, 1229–1241. https://doi.org/10.2151/jmsj.79.1229.

Lyon, B. and Camargo, S.J. (2009) The seasonally-varying influence of ENSO on rainfall and tropical cyclone activity in The Philippines. *Climate Dynamics*, 32, 125–141. https://doi.org/10.1007/s00382-008-0380-z.

Madden, R.A. and Julian, P.R. (1971) Detection of a 40–50-day oscillation in the tropics. *Journal of the Atmospheric Sciences*, 43, 3138–3158. https://doi.org/10.1175/1520-0469(1971)028<0702:DOADOI>2.0.CO;2.

Matsumoto, J. (1992) The seasonal changes in Asian and Australian monsoon regions. *Journal of the Meteorological Society of Japan*, 70, 257–273. https://doi.org/10.2151/jmsj1965.70.1B_257.

Matsumoto, J. (1995. Rainfall climatology over the asian monsoon region) In: Murai, S. Rainfall climatology over Asian monsoon region. (Ed.) *Toward Global Planning of Sustainable Use of the Earth*. Amsterdam: Elsevier.

Matsumoto, J. (1997) Seasonal transition of summer rainy season over Indochina and adjacent monsoon region. *Advances in Atmospheric Sciences*, 14, 231–245. https://doi.org/10.1007/s00376-997-0022-0.

Matsumoto, J., Olaguera, L.M., Nguyen-Le, D., Kubota, H. and Villafuerte, M.Q. (2020) Climatological seasonal changes of wind and rainfall in The Philippines. *International Journal of Climatology*, 1–15, 4843–4857. https://doi.org/10.1002/joc.6492.

Moron, V., Lucero, A., Hilario, F.D., Lyon, B., Robertson, A.W. and DeWitt, D. (2009) Spatio-temporal variability and predictability of summer monsoon onset over The Philippines. *Climate Dynamics*, 33, 1159–1177. https://doi.org/10.1007/s00382-008-0520-5.

Murakami, T. and Matsumoto, J. (1994) Summer monsoon over the Asian continent and western North Pacific. *Journal of the Meteorological Society of Japan*, 72, 719–745. https://doi.org/10.2151/jmsj1965.72.5_719.

Nakazawa, T. (1992) Seasonal phase lock of intraseasonal variation during the Asian summer monsoon. *Journal of the Meteorological Society of Japan*, 70, 597–611. https://doi.org/10.2151/jmsj1965.70.1B_597.

Olaguera, L.M. and Matsumoto, J. (2020) A climatological study of the wet and dry conditions in the pre-summer monsoon season of The Philippines. *International Journal of Climatology*, 40, 4203–4217. https://doi.org/10.1002/joc.6452.

Olaguera, L.M., Matsumoto, J., Kubota, H., Inoue, I., Cayanan, E.O. and Hilario, F.D. (2018a) Abrupt climate shift in the mature rainy season of The Philippines in the mid-1990s. *Atmosphere*, 9, 350. https://doi.org/10.3390/atmos9090350.

Olaguera, L.M., Matsumoto, J., Kubota, H., Inoue, I., Cayanan, E.O. and Hilario, F.D. (2018b) Interdecadal shifts in the winter monsoon rainfall of The Philippines. *Atmosphere*, 9, 464. https://doi.org/10.3390/atmos9120464.

Pullen, J., Gordon, A.L., Flatau, M., Doyle, J.D., Villanoy, C. and Cabrera, O. (2015) Multiscale influences on extreme winter rainfall in The Philippines. *Journal of Geophysical Research-Atmospheres*, 120, 3292–3309. https://doi.org/10.1002/2014JD022645.

Rajeevan, M., Gadgil, S. and Bhate, J. (2010) Active and break spells of the Indian summer monsoon. *Journal of Earth System Science*, 119, 229–247. https://doi.org/10.1007/s12040-010-0019-4.

Ramage, C.S. (1952) Variation of rainfall over South China through the wet season. *Bulletin of the American Meteorological Society*, 33, 308–311. https://doi.org/10.1175/1520-0477-33.7.308.

Ramage, C.S. (1971) *Monsoon Meteorology*. New York, NY: Academic Press.

Roberts, M.G., Dawe, D., Falcon, W.P. and Naylor, R.L. (2009) El Nino-southern oscillation impacts on rice production in Luzon, The Philippines. *Journal of Applied Meteorology and Climatology*, 48, 1718–1724. https://doi.org/10.1175/2008JAMC1628.1.

So, C.H. and Chan, J.C.L. (1997) Regional and synoptic-scale features associated with inactive periods of the summer monsoon over South China. *Advances in Atmospheric Sciences*, 14, 223–230. https://doi.org/10.1007/s00376-997-0021-1.

Takahashi, H. and Yasunari, T. (2006) A climatological monsoon break in rainfall over Indochina—a singularity in the seasonal march of the Asian summer monsoon. *Journal of Climate*, 19, 1545–1556. https://doi.org/10.1175/JCLI3724.1.

Tao, S. and Chen, L. (1987) A review of recent research on the East Asian summer monsoon in China. In: Chang, C.P. and Krishnamurti, T.N. (Eds.). *Monsoon Meteorology*. New York, NY: Oxford University Press.

Ueda, H. (2005) Air-sea coupled process involved in stepwise seasonal evolution of the Asian summer monsoon. *Geographical Review Japan*, 78, 825–841. https://doi.org/10.4157/grj.78.825.

Ueda, H. and Yasunari, T. (1996) Maturing process of the summer monsoon over the Western North Pacific: a coupled ocean/atmosphere system. *Journal of the Meteorological Society of Japan*, 74, 493–508 10.215/jmsj1965.74.4_493.

Ueda, H., Yasunari, T. and Kawamura, R. (1995) Abrupt seasonal change of large-scale convective activity over the western Pacific in the northern summer. *Journal of the Meteorological Society of Japan*, 73, 795–809. https://doi.org/10.2151/jmsj1965.73.4_795.

Wang, B., Ding, Q., Fu, X., Kang, I.S., Jin, K., Shukla, J. and Doblas-Reyes, F. (2005) Fundamental challenge in simulation and prediction of summer monsoon rainfall. *Geophysical Research Letters*, 32, L15711. https://doi.org/10.1029/2005GL022734.

Wang, B. and Xu, X. (1997) Northern Hemisphere summer monsoon singularities and climatological intra-seasonal oscillation. *Journal of Climate*, 10, 1071–1085. https://doi.org/10.1175/1520-0442(1997)010<1071:NHSMSA>2.0.CO;2.

Wu, R. (2002) Processes for the northeastward advance of the summer monsoon over the western North Pacific. *Journal of the Meteorological Society of Japan*, 80, 67–83. https://doi.org/10.2151/jmsj.80.67.

Wu, R. and Wang, B. (2000) Inter-annual variability of the summer monsoon onset over the western North Pacific and the underlying processes. *Journal of Climate*, 13, 2483–2501. https://doi.org/10.1175/1520-0442(2000)013<2483:IVOSMO>2.0.CO:2.

Wu, R. and Wang, B. (2001) Multi-stage onset of the summer monsoon over the western North Pacific. *Climate Dynamics*, 17, 277–289. https://doi.org/10.1007/s003820000118.

Yanai, M., Li, C. and Song, Z. (1992) Seasonal heating of the Tibetan plateau and its effects on the evolution of the Asian summer monsoon. *Journal of the Meteorological Society of Japan*, 70, 319–351. https://doi.org/10.2151/jmsj1965.70.1B_319.

Yumul, G.P., Cruz, N.A., Servando, N.T. and Dimalanta, C.B. (2011) Extreme weather events and related disasters in The Philippines, 2004-08: a sign of what climate change will mean? *Disasters*, 35, 362–382. https://doi.org/10.1111/j.1467-7717.2010.01216.x.

Zhang, Z., Chan, J.C.L. and Ding, Y. (2004) Characteristics, evolution, and mechanisms of the summer monsoon onset over Southeast Asia. *International Journal of Climatology*, 24, 1461–1482. https://doi.org/10.1002/joc.1082.

SUPPORTING INFORMATION

Additional supporting information may be found online in the Supporting Information section at the end of this article.

How to cite this article: Olaguera LMP, Matsumoto J, Kubota H, Cayanan EO, Hilario FD. A climatological analysis of the monsoon break following the summer monsoon onset over Luzon Island, Philippines. *Int J Climatol*. 2021;41: 2100–2117. https://doi.org/10.1002/joc.6949